Eur. Phys. J. E (2020) **43**: 67
DOI 10.1140/epje/i2020-11992-5

THE EUROPEAN PHYSICAL JOURNAL E

Regular Article

Negative friction memory induces persistent motion

Bernhard G. Mitterwallner[a], Laura Lavacchi, and Roland R. Netz

Fachbereich Physik, Freie Universität Berlin, 14195 Berlin, Germany

Received 25 May 2020 / Received in final form 6 September 2020 / Accepted 30 September 2020
Published online: 23 October 2020

Abstract. We investigate the mean-square displacement (MSD) for random motion governed by the generalized Langevin equation for memory functions that contain two different time scales: In the first model, the memory kernel consists of a delta peak and a single-exponential and in the second model of the sum of two exponentials. In particular, we investigate the scenario where the long-time exponential kernel contribution is negative. The competition between positive and negative friction memory contributions produces an enhanced transient persistent regime in the MSD, which is relevant for biological motility and active matter systems.

1 Introduction

If the dynamics of a diffusing particle is coupled to other degrees of freedom, memory effects occur, and the particle dynamics becomes non-Markovian [1,2]. Examples include the diffusion of a tracer bead in viscoleastic [3–6] and heterogeneous [7,8] media, polymer dynamics [9–13] and dynamics in rough energy landscapes [14–16]. Furthermore, many systems far from equilibrium, such as self-propelled particles [17–19] or passive tracer particles in active media [20–22], exhibit non-Markovian dynamics.

The random motion of a diffusing particle is commonly characterized by the mean-square displacement (MSD)

$$C_{\mathrm{MSD}}(t) = \left\langle (x(t) - x(0))^2 \right\rangle . \tag{1}$$

Diffusive properties may be classified in terms of the time-dependent MSD exponent $\alpha(t)$:

$$\alpha(t) = \frac{\mathrm{d}\ln C_{\mathrm{MSD}}(t)}{\mathrm{d}\ln t} . \tag{2}$$

Normal diffusion (Brownian motion) yields an exponent $\alpha = 1$. Processes for which $\alpha \neq 1$ are broadly referred to as anomalous diffusion, or more specifically, subdiffusion for $\alpha < 1$ and superdiffusion for $\alpha > 1$. Much effort has been directed towards modeling anomalous diffusion especially for cases in which the exponent stays anomalous in the long-time limit, for recent reviews see [23,24]. In many instances, however, the dynamics becomes effectively Markovian at long time scales, which leads to normal diffusion, *i.e.* $\alpha = 1$, for $t \to \infty$. The MSD of an underdamped particle (or a reaction coordinate with a non-vanishing effective mass) is ballistic, *i.e.* persistent, at short times ($\alpha = 2$). The crossover between the persistent and the diffusive regimes generally depends on details of the non-Markovian dynamics, which are relevant at short and intermediate time scales [25].

The generalized Langevin equation (GLE) offers a convenient framework for the description of non-Markovian dynamics by introducing a memory term in the equation of motion. It has been successfully applied to passive microrheology [4–6], the modeling of (bio-)molecular systems [14, 26–30] and for the investigation of non-Markovian effects on barrier-crossing dynamics [31, 32]. In one dimension, the GLEs for the underdamped (UD) and overdamped (OD) cases read [33]:

$$\ddot{x}(t) = -\int_0^\infty \Gamma(t')\dot{x}(t-t')\mathrm{d}t' + F_R(t) \quad \text{(UD)}, \tag{3}$$

$$0 = -\int_0^\infty \Gamma(t')\dot{x}(t-t')\mathrm{d}t' + F_R(t) \quad \text{(OD)}. \tag{4}$$

In our notation, $F_R(t)$ denotes the random force with zero mean and $\Gamma(t)$ is the symmetric memory kernel obeying

$$\int_0^\infty \Gamma(t)\mathrm{d}t = \frac{1}{\tau_m} , \qquad \Gamma(t) = \Gamma(-t). \tag{5}$$

For cases in which eq. (3) describes the dynamics of a massive particle, the acceleration term, $\ddot{x}(t)$, normally has the particle mass m as a prefactor. Here, the mass has been absorbed into $\Gamma(t)$ and $F_R(t)$. The integral of the kernel must be positive and sets the characteristic time scale τ_m which, for a massive particle moving in a viscoelastic medium, is the inertial time scale given by the ratio of its mass and the total friction. We shall consider equilibrium systems for which the fluctuation-dissipation

[a] e-mail: bmitt@zedat.fu-berlin.de

theorem holds [33], which implies that the autocorrelation of the random force $F_R(t)$ is proportional to the memory kernel

$$\langle F_R(t)F_R(0)\rangle = B\Gamma(t). \tag{6}$$

In the underdamped case, B is the mean-squared velocity of the particle, see appendix A. If the kernel is short-ranged, the dynamics becomes Markovian at large time scales and exhibits normal diffusion, while long-ranged kernels may lead to anomalous diffusion on arbitrarily long time scales [34]. Equation (6) together with the Wiener-Khinchin theorem implies that the power spectrum of the random force F_R is proportional to the frequency-domain symmetric memory kernel. Thus the frequency-domain kernel must be non-negative (assuming $B > 0$), which is an important constraint on its functional form. This is of particular importance in the case of negative long-time memory tails, as will be discussed in detail later on and in appendix B.

In this work, we investigate GLEs with memory kernels comprised of either a single-exponential and a delta contribution or two exponentials. These two models have previously been employed, in particular to model tracer particle motion in viscoelastic media [5,6,35]. Here we take a more general perspective and explore a new parameter regime in which the kernel is positive for short times and has a negative tail, such that the kernel stays positive everywhere in the frequency domain. For both the overdamped and underdamped cases, we show that these competing contributions to the memory kernel lead to a transient persistent regime in the MSD. Transient persistent motion appears in various models for self-propelled particles [17–19], transient dynamics of sheared systems [36,37] and single-cell motility [38]. Interestingly, the connection to negative memory contributions has been previously noted in the last two examples. Here we systematically investigate how an equilibrium description in terms of a GLE with negative memory contribution captures transient persistent motion.

2 Free active particle models

As a first example, we consider the model of a run-and-tumble particle (RTP) [18, 39] in $d = 2$ spatial dimensions. The particle moves at constant speed $|\vec{u}(t)| = v_0$ in a given direction ("run") and then instantaneously reorients and chooses a random new direction ("tumble") from a uniform distribution over $[0, 2\pi)$. Reorientations occur at a rate $1/\tau_p$ and thus $\langle\vec{u}(t)\vec{u}(0)\rangle = v_0^2 e^{-|t|/\tau_p}$. Additionally, the particle velocity is subject to thermal fluctuations $\sqrt{D_0}\vec{\xi}(t)$, which are modeled as zero-mean, white Gaussian noise, *i.e.* $\langle\vec{\xi}(0)\vec{\xi}(t)\rangle = 2d\delta(t)$. The total particle velocity is then given as the sum of two contributions

$$\dot{\vec{x}}(t) = \vec{u}(t) + \sqrt{D_0}\vec{\xi}(t), \tag{7}$$

which leads to the corresponding MSD [18, 40]

$$\begin{aligned} C_{\mathrm{MSD}}(t) &= \frac{1}{d}\left\langle(\vec{x}(t) - \vec{x}(0))^2\right\rangle \\ &= 2\left(D_0 + \frac{v_0^2\tau_p}{d}\right)t + \frac{2v_0^2\tau_p^2}{d}\left(e^{-t/\tau_p} - 1\right). \end{aligned} \tag{8}$$

From eq. (8) it can be seen that the motion is diffusive at long times with an effective diffusion constant $D = D_0 + v_0^2\tau_p/d$, while for short times, it is also diffusive but characterized by the diffusion constant D_0, the overall particle dynamics thus is overdamped. Figure 1(a) shows simulated sample trajectories of a run-and-tumble particle. The corresponding MSD, eq. (8), which exhibits a transient persistent regime, is shown as a solid black line in fig. 1(c).

As a second example, we consider the underdamped version of the active Ornstein-Uhlenbeck particle (AOUP) [19, 41–43]. Its equations of motion read in d dimensions

$$\begin{aligned} \tau_p\dot{\vec{u}}(t) &= -\vec{u}(t) + v_0\sqrt{\frac{\tau_p}{d}}\vec{\xi}_u(t), \\ \tau_b\ddot{\vec{x}}(t) &= -\dot{\vec{x}}(t) + \vec{u}(t) + \sqrt{D_0}\vec{\xi}(t), \end{aligned} \tag{9}$$

where $\vec{\xi}(t)$ and $\vec{\xi}_u(t)$ are again zero-mean, white Gaussian noise with $\langle\vec{\xi}(t)\vec{\xi}(t')\rangle = \langle\vec{\xi}_u(t)\vec{\xi}_u(t')\rangle = 2d\delta(t-t')$ and $\langle\vec{\xi}(t)\vec{\xi}_u(t')\rangle = 0$. Figure 1(b) shows sample trajectories of an underdamped AOUP in $d = 2$ dimensions which were generated with the method described in appendix C. $\vec{u}(t)$ is an Ornstein-Uhlenbeck process and has the solution

$$\vec{u}(t) = \frac{v_0^2}{\sqrt{d\tau_p}}\int_{-\infty}^{t} \mathrm{d}t' e^{-(t-t')/\tau_p}\vec{\xi}_u(t') \tag{10}$$

and thus has an exponential autocorrelation function, *i.e.* $\langle\vec{u}(t)\vec{u}(0)\rangle = v_0^2 e^{-|t|/\tau_p}$, while the magnitude $|\vec{u}(t)|$ is not fixed. The MSD is then given by [38]

$$\begin{aligned} C_{\mathrm{MSD}}(t) = 2&\left(D_0 + \frac{v_0^2\tau_p}{d}\right)t \\ &+2\left(D_0\tau_b - \frac{v_0^2\tau_p\tau_b^3}{d(\tau_p^2 - \tau_b^2)}\right)\left(e^{-t/\tau_b} - 1\right) \\ &+\frac{2v_0^2\tau_p^4}{d(\tau_p^2 - \tau_b^2)}\left(e^{-t/\tau_p} - 1\right). \end{aligned} \tag{11}$$

Except for the initial persistent regime at short times $t < \tau_b$, the MSD is the same as for the RTP, see fig. 1(c), where the MSD of the AOUP is shown as a red broken line. Note that the difference of the MSD at short times stems from the fact that the dynamics for the RTP is assumed overdamped, while the AOUP that we consider obeys underdamped dynamics.

Given the velocity autocorrelation function $\langle\dot{\vec{x}}(t)\dot{\vec{x}}(0)\rangle$, the memory kernel may be extracted numerically, see [26, 44–46] and appendix D. The method finds the kernel for which eq. (6) holds and thus maps a given MSD to its corresponding effective equilibrium

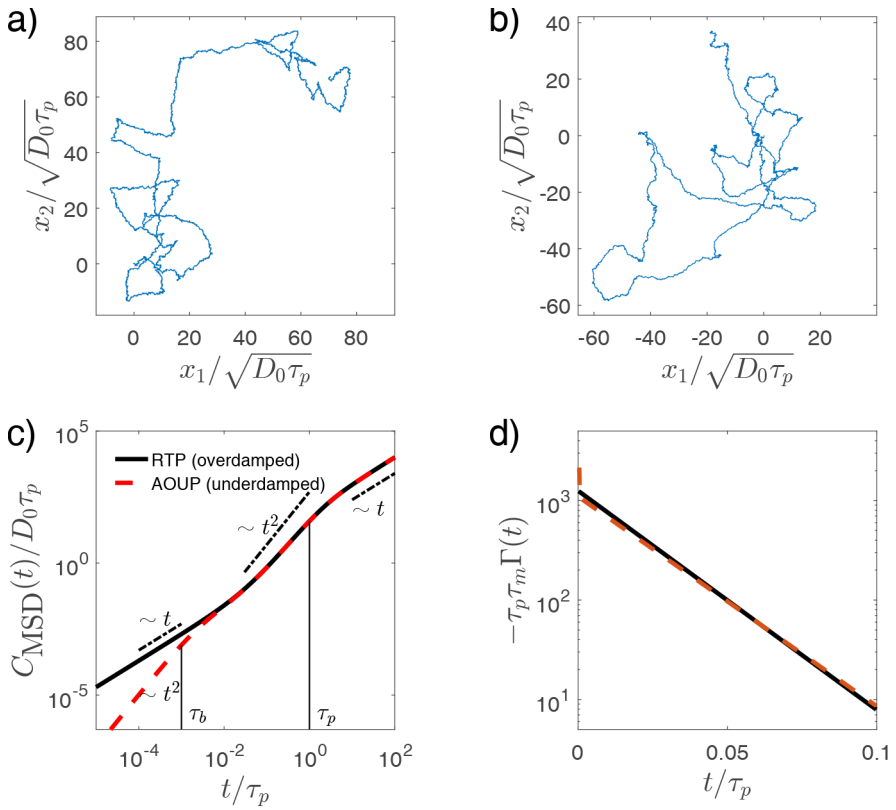

Fig. 1. (a), (b): sample trajectories of length $50\tau_p$ for free active particles in $d = 2$ dimensions for $v_0 = 10\sqrt{D_0/\tau_p}$. (a) Run-and-tumble particle simulated with a time step $\Delta = 10^{-3}\tau_p$. (b) Underdamped active Ornstein-Uhlenbeck particle simulated for $\tau_b = 10^{-3}\tau_p$ with a time step $\Delta = 10^{-4}\tau_p$. (c) MSDs corresponding to the run-and-tumble particle (solid black line) and the underdamped AOUP (dashed red line), see eqs. (8) and (11), respectively. (d) Kernels extracted from the MSDs shown in (c). Both show the same structure of a positive delta peak at $t = 0$ followed by a negative exponential tail.

GLE [38]. For the two examples shown in fig. 1, this means that the equations of motion for the underdamped AOUP, eq. (9), and the RTP, eq. (7) are mapped onto the under- and overdamped GLEs, eq. (3) and eq. (4), respectively. Such a mapping onto a substitute Gaussian model reproduces all two-point correlation functions but fails to capture the full non-linear dynamics of a non-Gaussian process such as the RTP. However, for the purpose of our work, this limitation is not important since we are interested in how features in the MSD, which is a two-point correlation function, are connected to properties of the substitute kernel.

For both examples, the numerically extracted kernel has the same structure, consisting of an initial positive delta peak (not shown) followed by a negative exponential tail, see fig. 1(d). The observation that kernels with negative tails lead to transient persistent regimes in the MSD forms the motivation for the present work. The nature of the different regimes in the MSD and the interplay of over- and underdamped dynamics with memory effects will be illustrated by phase diagrams of the MSD exponent α as a function of relevant system parameters.

3 General considerations

In the frequency domain, the solution of both the over- and underdamped GLE, eq. (4) and eq. (3), can be written in terms of the position response function $\tilde{\chi}(\omega)$, which is defined via

$$\tilde{x}(\omega) = \tilde{\chi}(\omega)\tilde{F}_R(\omega). \tag{12}$$

Introducing $\Gamma_+(t) := \Theta(t)\Gamma(t)$, the response function $\tilde{\chi}(\omega)$ for the over- and underdamped case, respectively, is given by

$$\tilde{\chi}(\omega) = \frac{1}{-\omega^2 + i\omega\tilde{\Gamma}_+(\omega)} \quad \text{(UD)}, \tag{13}$$

$$\tilde{\chi}(\omega) = \frac{1}{i\omega\tilde{\Gamma}_+(\omega)} \quad \text{(OD)}. \tag{14}$$

We use the convention $\tilde{f}(\omega) = \int_{-\infty}^{\infty} \mathrm{d}t e^{-i\omega t} f(t)$ for the Fourier transform of a function $f(t)$. Using eq. (6), the position autocorrelation function $C_{xx}(t) = \langle x(t)x(0)\rangle$ in Fourier space reads

$$\tilde{C}_{xx}(\omega) = B\tilde{\Gamma}(\omega)\tilde{\chi}(\omega)\tilde{\chi}(-\omega). \tag{15}$$

By noting that

$$\begin{aligned}\tilde{\chi}(-\omega) - \tilde{\chi}(\omega) &= i\omega\left(\tilde{\Gamma}_+(\omega) + \tilde{\Gamma}_+(-\omega)\right)\tilde{\chi}(\omega)\tilde{\chi}(-\omega) \\ &= i\omega\tilde{\Gamma}(\omega)\tilde{\chi}(\omega)\tilde{\chi}(-\omega),\end{aligned} \tag{16}$$

eq. (15) may be rewritten as

$$\tilde{C}_{xx}(\omega) = \frac{B}{i\omega}\left[\tilde{\chi}(-\omega) - \tilde{\chi}(\omega)\right]. \tag{17}$$

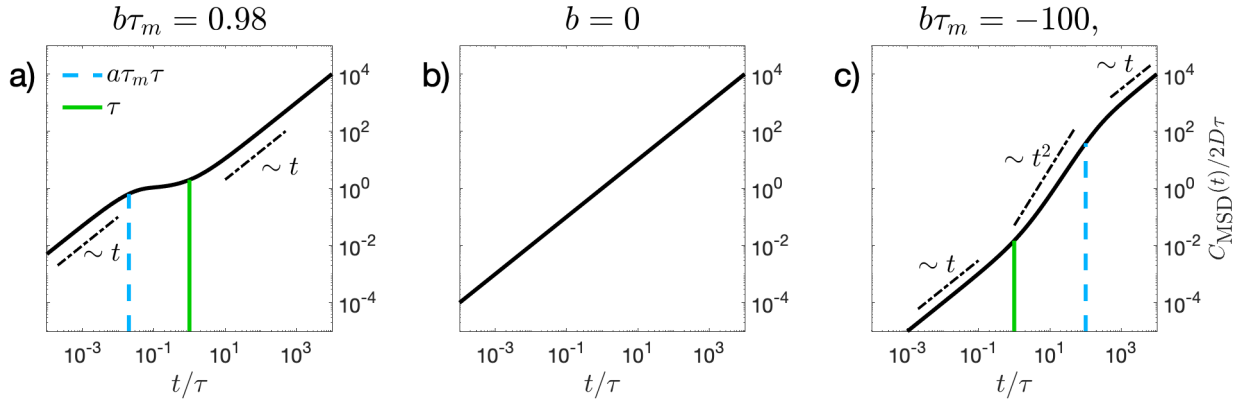

Fig. 2. Overdamped motion in the presence of delta-exponential memory, see eq. (20). The MSD has two diffusive regimes for $b\tau_m \neq 0$ and the crossover region between them is a plateau for $0 < b\tau_m < 1$ and a persistent regime for $b\tau_m < 0$. The case $b = 0$ corresponds to the Markovian case of simple Brownian motion with exponent $\alpha = 1$.

The MSD is then given by

$$C_{\mathrm{MSD}}(t) = 2C_{xx}(0) - 2C_{xx}(t) = B\int_{-\infty}^{\infty} \frac{\mathrm{d}\omega}{\pi} \frac{e^{i\omega t} - 1}{i\omega} \left[\tilde{\chi}(\omega) - \tilde{\chi}(-\omega)\right]. \quad (18)$$

Note that using the above formula, $C_{\mathrm{MSD}}(0) = 0$ is automatically fulfilled [6,47]. The long-time diffusion constant D is determined by the contribution from the simple pole at $\omega = 0$ in the integrand of eq. (18)

$$D = \lim_{t\to\infty} \frac{C_{\mathrm{MSD}}(t)}{2t} = B\tau_m, \quad (19)$$

where we used that $\tilde{\Gamma}_+(0) = 1/\tau_m$, which follows from eq. (5). In the overdamped case, B and τ_m are not uniquely defined and can be chosen freely as long as eq. (19) holds. For a given diffusion constant D together with the rescaled kernel $\tau_m\Gamma(t)$, the overdamped dynamics is then uniquely determined.

4 Delta-exponential memory

Motivated by the result shown in fig. 1(d), we consider a memory kernel which is given by the sum of a delta peak and a single-exponential

$$\Gamma(t) = 2a\delta(t) + \frac{b}{\tau} e^{-|t|/\tau}. \quad (20)$$

The two amplitudes a and b set the time scale $\tau_m = 1/(a + b)$. We will refer to the model eq. (20) simply as delta-exponential kernel. We restrict our considerations to the case of a positive contribution from the delta peak, *i.e.* $a > 0$. Together with $a + b > 0$, this is a sufficient condition so that the kernel is positive in the frequency domain, see appendix B, and furthermore that the corresponding response function is causal, *i.e.* that it is single-sided in the time domain, $\chi(t < 0) = 0$. The latter implies that $\tilde{\chi}(\omega)$ has no poles in the lower half complex plane. This model may be regarded as a general ansatz for exponentially decaying kernels for which only the slowest decaying mode can be resolved in time. Other features of the kernel that decay on shorter time scales are therefore absorbed into the delta contribution.

First, we consider the overdamped case: We obtain the following expressions for the response function and the MSD, respectively [6]:

$$\tilde{\chi}(\omega)/\tau_m = \frac{1 + i\omega\tau}{-\omega a\tau_m\tau(\omega - i/a\tau_m\tau)}, \quad (21)$$

$$C_{\mathrm{MSD}}(t)/2D = t - b\tau_m\tau\left(e^{-t/a\tau_m\tau} - 1\right). \quad (22)$$

The expression in eq. (21) has a pole at $i/a\tau_m\tau$ and thus a must be positive for the response to be causal. Figure 2 shows the corresponding MSD which exhibits a crossover region between the two characteristic time scales τ and $a\tau_m\tau$: For positive tails $b > 0$, the crossover region is a plateau, *i.e.* the particle is subject to a transient confinement effect. For negative tails $b < 0$, the crossover region is a persistent regime, which is the same behavior observed for the active particle models in fig. 1(c).

More generally, the dynamics may be underdamped, which leads to persistent motion at the shortest times $t \to 0$ and a non-trivial interplay between inertial and memory effects [6]. The response function of the underdamped case is given by

$$\tilde{\chi}(\omega) = \frac{1 + i\omega\tau}{i\omega(-\tau\omega^2 + i\omega(1 + a\tau) + a + b)}. \quad (23)$$

Note that for a positive delta peak in the kernel, *i.e.* $a > 0$, together with the condition $\tau_m^{-1} = a + b > 0$, the response eq. (23) has no poles in the lower half-plane and is thus causal. We obtain for the MSD [6]

$$C_{\mathrm{MSD}}(t)/2D = t + \frac{\tau_b(\tau - \tau_b)}{\tau_p - \tau_b}\left(e^{-t/\tau_b} - 1\right) + \frac{\tau_p(\tau_p - \tau)}{\tau_p - \tau_b}\left(e^{-t/\tau_p} - 1\right), \quad (24)$$

$$\tilde{\chi}(\omega)/\tau_m = \frac{(1+i\omega\tau_1)(1+i\omega\tau_2)}{i\omega[-a_0\tau_m\tau_1\tau_2\omega^2 + i\omega\tau_m(a_0(\tau_1+\tau_2)+a\tau_2+b\tau_1)+a_0\tau_m+1]}\,. \tag{32}$$

with the characteristic time scales

$$\tau_{b,p} = \frac{1+a\tau \pm \sqrt{(1+a\tau)^2 - 4\tau(a+b)}}{2(a+b)}\,, \tag{25}$$

where we choose the positive sign for τ_p. We obtain the following asymptotic behavior:

$$\tau_b = \begin{cases} 1/a, & \tau \to \infty, \\ \tau + \mathcal{O}(\tau^2), & \tau \to 0, \end{cases} \tag{26}$$

$$\tau_p = \begin{cases} a\tau_m\tau + \mathcal{O}(1), & \tau \to \infty, \\ \tau_m, & \tau \to 0. \end{cases} \tag{27}$$

For large memory times τ, the motion is persistent at the shortest times up to the time scale $\tau_b = 1/a$, which is given by the delta contribution of the kernel. τ_p approaches $a\tau_m\tau$ for large τ, which recovers the characteristic time scale in the MSD (22) of the overdamped solution.

If the kernel is positive everywhere, *i.e.* $a, b > 0$, oscillations may occur in the MSD [6]. In fact, for $\tau_- < \tau < \tau_+$ with

$$\tau_\pm = \left(\sqrt{a+b} \mp \sqrt{b}\right)^{-2} \tag{28}$$

and $a, b > 0$, the time scales $\tau_{b,p}$ pick up a non-vanishing imaginary part. For the case $a \to 0$, which corresponds to the case of a memory kernel comprised of a single-exponential only, τ_+ diverges and thus there is an oscillatory regime in the MSD for all memory times $\tau > \tau_-$.

For negative exponential tails of the kernel, *i.e.* $b < 0$, there are no oscillations in the MSD. For very pronounced negative tails and long memory times, *i.e.* $b\tau_m \ll -1$ and $\tau \gg \tau_m$, we obtain the following scaling regimes in the MSD [38]:

$$C_{\mathrm{MSD}}(t) \sim \begin{cases} t^2, & t \ll 1/a, \\ t, & 1/a \ll t \ll \tau, \\ t^2, & \tau \ll t \ll a\tau_m\tau, \\ t, & a\tau_m\tau \ll t. \end{cases} \tag{29}$$

The columns in fig. 3 show results for three exemplary cases of negative, zero and positive exponential tails of the kernel. For a fixed memory time $\tau = 10^5\tau_m$, figs. 3(a)–(c) and (d)–(f) show simulated trajectories and the corresponding analytical MSDs, respectively. The case $b = 0$ corresponds to the Markovian case of a standard persistent random walk. For positive (negative) exponential tails of the kernel, *i.e.* $b > 0$ ($b < 0$), the dynamics exhibit transient confinement (persistent motion) in between the initial persistent motion at short times and diffusion at long times. Figures 3(g)–(i) show the MSD exponent α as a function of time t and memory time τ. The characteristic time scales τ_b and τ_p are shown as dotted and dashed lines, respectively. In particular, the duration τ_b of the initial persistent motion increases (decreases) for positive (negative) tails. The oscillatory regime for positive kernels with memory times $\tau_- < \tau < \tau_+$ can be seen in fig. 3(g).

5 Bi-exponential memory

In a more general scenario, both contributions to the memory kernel are given by exponentials

$$\Gamma(t) = \frac{a}{\tau_1}e^{-|t|/\tau_1} + \frac{b}{\tau_2}e^{-|t|/\tau_2}\,. \tag{30}$$

This model describes the situation in which the shortest time scale can be resolved in time and/or when the two time scales τ_1 and τ_2 are not necessarily separated. The kernel is positive in the frequency domain, if the shorter mode of the kernel is positive, *i.e.* $\tau_2 > \tau_1$ for $a > 0$ and vice versa, see appendix B.

The treatment of the overdamped case for kernels solely comprised of exponentials with finite memory times requires special care, since the overdamped limit is singular [5,6]. As discussed in detail in [6], the problem can be regularized via the addition of a positive delta contribution to the kernel. For the treatment of the overdamped case, we shall therefore consider the extended kernel

$$\Gamma(t) = 2a_0\delta(t) + \frac{a}{\tau_1}e^{-|t|/\tau_1} + \frac{b}{\tau_2}e^{-|t|/\tau_2}. \tag{31}$$

The corresponding response function is then given by

see eq. (32) *above*

For the constraints on the kernel parameters mentioned earlier and $a_0 > 0$, the response function eq. (32) is causal. Doing the back transform, eq. (18), and then taking the limit $a_0 \to 0$ for $t > 0$, we obtain the MSD [6]

$$C_{\mathrm{MSD}}(t>0)/2D = t + \frac{\tau_1\tau_2}{\tau'} + \frac{(\tau'-\tau_1)(\tau'-\tau_2)}{\tau'}\left(e^{-t/\tau'} - 1\right), \tag{33}$$

where we have introduced the time scale

$$\tau' = \frac{b\tau_1 + a\tau_2}{a+b} = (a\tau_2 + b\tau_1)\tau_m. \tag{34}$$

For the case in which the memory times are separated, *e.g.* $\tau_2 \gg \tau_1$, we have $\tau' \approx a\tau_m\tau_2$, which recovers the characteristic time scale of the overdamped delta-exponential case. The MSD is constant at short times $t \ll \tau_1\tau_2/\tau'$ for all cases. This transient effective confinement may be explained by the force created by the more short-ranged kernel contribution and is the main difference to the underdamped case of the delta-exponential kernel for which the MSD is ballistic at short times. Note that the correct initial condition, $C_{\mathrm{MSD}}(0) = 0$ is still fulfilled and the

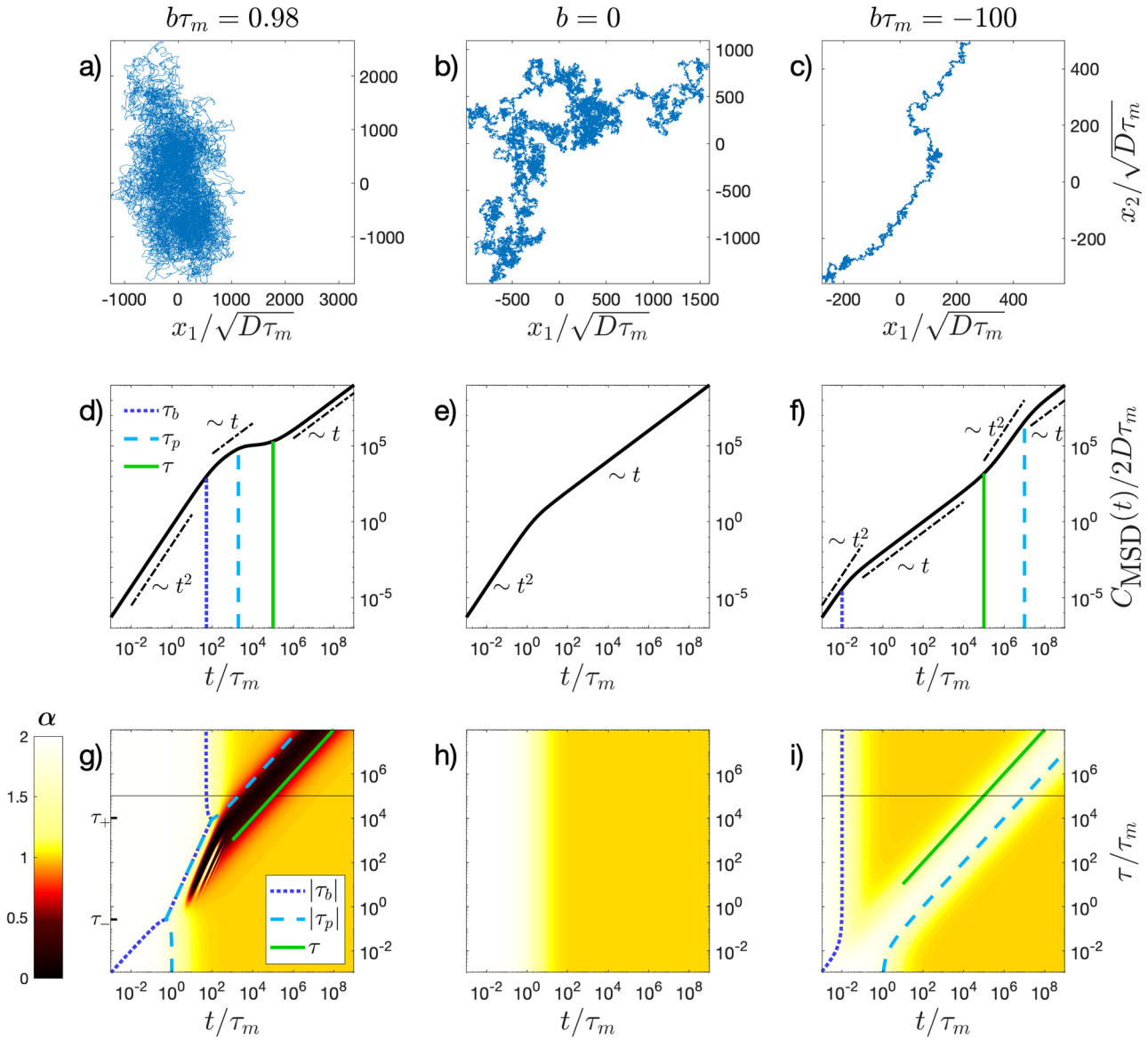

Fig. 3. Underdamped motion for three exemplary cases of negative, zero and positive exponential tail of the delta-exponential kernel eq. (20). Panels (a)–(c) show sample trajectories in 2D: the $x_1(t)$ and $x_2(t)$ components are solutions of eq. (3) where the random force has Gaussian statistics. The sample trajectories were generated with a timestep of $\Delta = 10\tau_m$, (see appendix C), and are of length of the memory time τ, which is set to $\tau = 10^5\tau_m$. (d)–(f) Analytical MSDs according to eq. (24) corresponding to the trajectories shown in (a)–(c). (g)–(i) Phase diagrams of the MSD exponent α as a function of time t and memory time τ. For a positive tail of the kernel, see (g), the time scales $\tau_{b,p}$ may pick up an imaginary part for $\tau_- < \tau < \tau_+$ and their absolute values are shown in this case. Cuts through the diagrams for $\tau = 10^5\tau_m$, *i.e.* the cases corresponding to the examples (a)–(f) are denoted by horizontal black lines.

MSD has a jump at $t = 0$. Figure 4 shows phase diagrams of the MSD exponent α. For negative kernels, *i.e.* $b < 0$, the phase diagram is only shown for the region in which $\tau_2 > \tau_1$, which must hold in order to satisfy causality.

For the underdamped case, we consider the unregularized bi-exponential kernel eq. (30) and the back-transform in eq. (18) is done numerically. If the memory times are separated and one of them is very large, say $\tau_2 \gg \tau_1 \approx \tau_m$, the expression for the response function simplifies for the long- and short-time limits [6]: For long times, where t is comparable to τ_2, we have $\omega \approx 1/\tau_2$ and the response function can be approximated by

$$\tilde{\chi}(\omega) \approx \frac{a\tau_2(1 + i\omega\tau_2)}{-\omega[\omega - i/a\tau_m\tau_2]} . \tag{35}$$

From the poles we obtain the characteristic time scale $a\tau_m\tau_2$, similar to the delta-exponential case.

We study the initial persistent regime by considering times t comparable to $\tau_1 \approx \tau_m$ and thus $\omega \gg 1/\tau_2$. In this

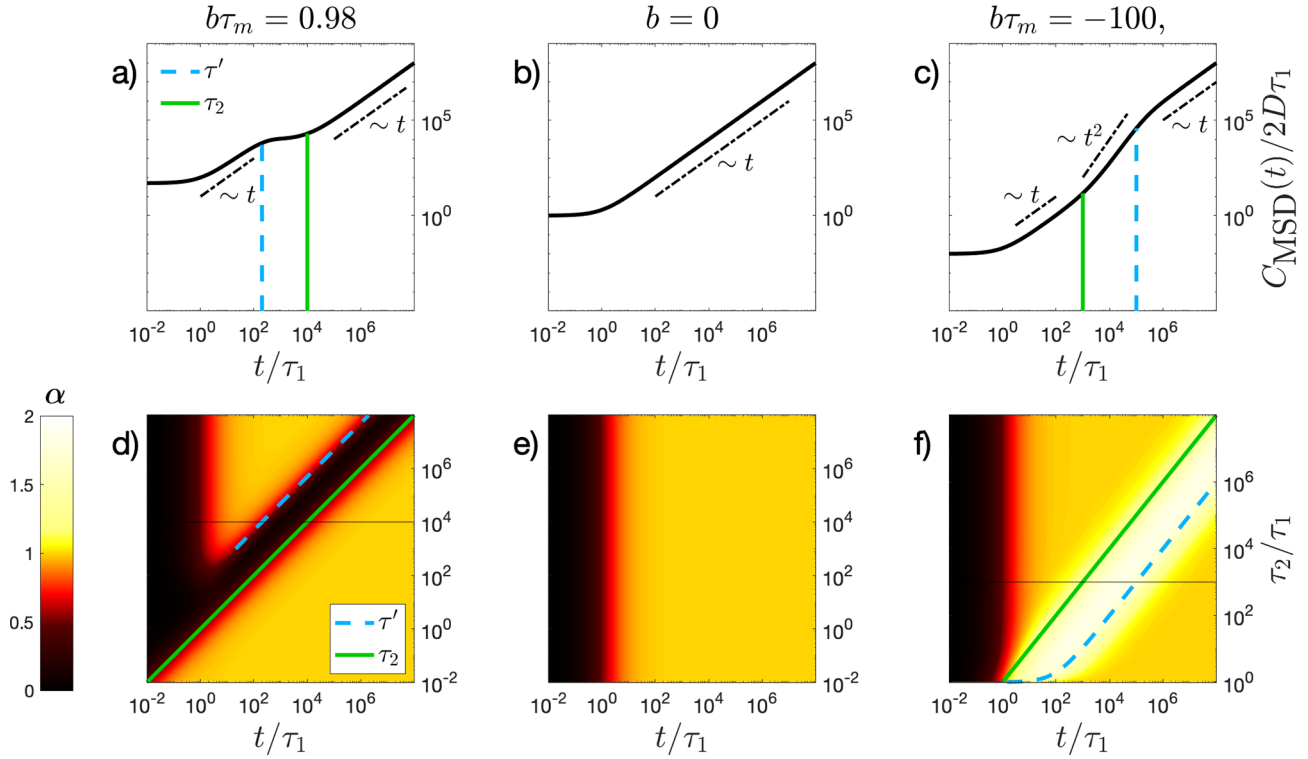

Fig. 4. Overdamped motion in the presence of bi-exponential memory eq. (31) and in the limit $a_0 \to 0$. The introduction of an additional time scale τ_1 leads to transient effective confinement, *i.e.* a constant MSD, at short times in contrast to the case of delta-exponential memory, cf. fig. 2. The phase diagram (f) for the negative tail ($b\tau_m = -100$) is only shown for $\tau_2 > \tau_1$, so that the shorter exponential kernel contribution is always positive.

case the response function can be approximated by

$$\tilde{\chi}(\omega) \approx \frac{1 + i\omega\tau_1}{i\omega[-\omega^2\tau_1 + i\omega + a]}, \tag{36}$$

with poles

$$\omega_\pm = \frac{i}{2\tau_1} \pm \sqrt{-\frac{1}{4\tau_1^2} + \frac{a}{\tau_1}}. \tag{37}$$

The initial persistent regime ends at $\tau'' := 1/|\omega_+|$. For $a > 1/4\tau_1$ the expression in eq. (37) picks up a non-vanishing real part and thus oscillations occur in the MSD which decay with a characteristic time $2\tau_1$. Since $a+b = 1/\tau_m > 0$ must hold, it follows that $a \gg 1/\tau_m$ for very pronounced negative tails. We thus obtain in the asymptotic case $\tau_2 \gg \tau_1 \approx \tau_m$ the following scaling of the MSD for negative b:

$$C_{\mathrm{MSD}}(t) \sim \begin{cases} t^2, & t \ll \sqrt{\tau_1/a}, \\ \text{oscillating}, & \sqrt{\tau_1/a} \ll t \ll 2\tau_1, \\ t, & 2\tau_1 \ll t \ll \tau_2, \\ t^2, & \tau_2 \ll t \ll a\tau_m\tau_2, \\ t, & a\tau_m\tau_2 \ll t. \end{cases} \tag{38}$$

Figure 5 shows phase diagrams of the MSD exponent α for $\tau_1 = \tau_m$, *i.e.* for the case in which the inertial time scale is equal to one of the memory times. The behavior is similar to the underdamped case of delta-exponential memory, see eq. (29). The positive (negative) tail of the kernel leads to transient confinement (transient persistent motion) at intermediate time scales $a\tau_m\tau_2 < t < \tau_2$ ($\tau_2 < t < a\tau_m\tau_2$). The case of $b = 0$ corresponds to a single-exponential kernel, which is analogous to a massive particle diffusing in a single-mode Maxwell fluid [47]. For our choice of parameters, oscillations occur in the MSD exponent, which are however barely discernible, see fig. 5(e). As mentioned earlier, for the integral over the kernel to stay positive, a negative tail needs to be compensated for by a larger amplitude of the positive shorter mode, which then acts as a strong confining force at shorter time scales. Together with the initial persistence (inertial effects, in case of a massive particle), and in the absence of any damping force, this then gives rise to pronounced oscillations at short times, see fig. 5(c) and (f).

6 Conclusion

We have investigated the MSD for random motion of a particle governed by the GLE for two different memory scenarios, namely for a memory kernel comprised of a delta peak and a single-exponential mode and for a memory kernel comprised of a bi-exponential kernel. For both the over- and underdamped cases, we have explored the parameter regime where the kernel has a negative tail. We find that such kernels give rise to a transient persistent regime in the MSD, which is a prominent feature of many

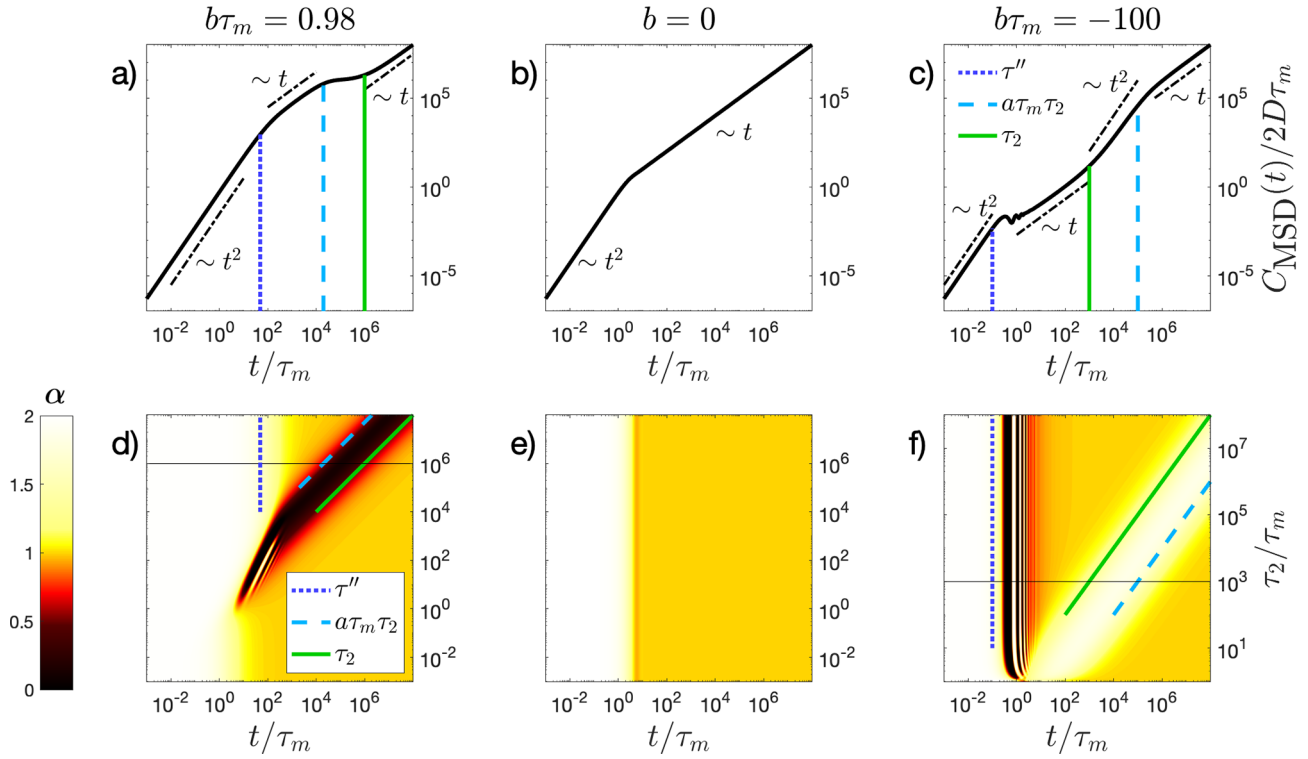

Fig. 5. Underdamped motion in the presence of bi-exponential memory, eq. (30), for $\tau_1 = \tau_m$. The notable difference to the underdamped delta-exponential model (see fig. 3) is the occurrence of oscillations for a negative tail of the kernel ($b < 0$). For large lag times t, the crossover is described by the characteristic time scales τ_2 and $a\tau_m\tau_2 \approx \tau'$.

random walk models for self-propelled particles, see fig. 1. We only treat the linear GLE with Gaussian random noise, which gives rise to purely Gaussian behavior, and therefore cannot describe possible non-Gaussian properties of active or passive particle models.

Memory kernels with negative tails may arise in purely equilibrium systems. For instance, the contribution from hydrodynamic back-flow to the dynamics of a spherical colloid immersed in a solvent gives rise to a negative power-law tail in the corresponding memory kernel [29, 48, 49]. The negative-tailed delta-exponential kernel discussed in this work also describes the dynamics of a particle whose velocity is coupled to a hidden degree of freedom, while the overall system remains in equilibrium [50].

On the level of two-point correlation functions, such as the MSD, an (effective) equilibrium description may be obtained for a single degree of freedom by finding the corresponding kernel $\Gamma(t)$ [26, 44, 46]. This has been of relevance for the interpretation of single particle tracking data of systems in and out of equilibrium where often only single, non-coupled degrees of freedom can be tracked [35, 38, 51].

The models for self-propelled particles discussed in the introduction are out of equilibrium, as are many experimentally relevant systems such as motile cells and tracer particles in active media. Given the trajectory for a single Gaussian degree of freedom, unambiguous extraction of the underlying non-equilibrium dynamics is not possible, while the observed dynamics may be fully described by an effective equilibrium-like substitute model. Interestingly, these effective descriptions have led to memory kernels with negative tails [38], which might suggest the interpretation that energy is injected into the system at intermediate time scales. We anticipate that our results will be of further relevance for the analysis of single-particle tracking data of active systems.

Open Access funding enabled and organized by Projekt DEAL. We acknowledge insightful discussions with Jan O. Daldrop and Felix Höfling. This project has received funding from the European Union's Horizon 2020 research and innovation program under grant agreement No. 674979-NANOTRANS, from the DFG SFB 1114 in project B2 and from the European Research Council (ERC) under the European Union's Horizon 2020 research and innovation program under grant agreement No. 835117.

Author contribution statement

RRN and BGM designed the project. BGM, LL and RRN performed research. BGM and RRN wrote the paper.

Appendix A. Velocity autocorrelation function

The GLE, eq. (3), for an underdamped particle can be written in terms of the velocity $v(t) = \dot{x}(t)$:

$$\dot{v}(t) = -\int_{-\infty}^{t} \mathrm{d}t' \Gamma(t-t')v(t') + F_R(t). \tag{A.1}$$

The corresponding velocity response defined via $\tilde{v}(\omega) = \tilde{\chi}_v(\omega)\tilde{F}_R(\omega)$ reads in the frequency domain:

$$\tilde{\chi}_v(\omega) = \frac{1}{i\omega + \tilde{\Gamma}_+(\omega)}\,. \tag{A.2}$$

By noting that $\tilde{\Gamma}(\omega)\tilde{\chi}_v(\omega)\tilde{\chi}_v(-\omega) = \tilde{\chi}_v(\omega) + \tilde{\chi}_v(-\omega)$, the velocity autocorrelation function (VACF), $C_{vv}(t) = \langle v(t)v(0)\rangle$ can be written in the frequency domain as

$$\tilde{C}_{vv}(\omega) = B\tilde{\chi}_v(\omega) + B\tilde{\chi}_v(-\omega). \tag{A.3}$$

From this, we obtain an expression for the diffusion constant D, via the Green-Kubo relation

$$D = \int_0^\infty \mathrm{d}t C_{vv}(t) = \frac{\tilde{C}_{vv}(0)}{2} = B\tau_m, \tag{A.4}$$

in agreement with eq. (19).

The mean-squared velocity is given by

$$\begin{aligned}\langle v(t)^2\rangle = C_{vv}(0) &= \int_{-\infty}^{\infty}\frac{\mathrm{d}\omega}{2\pi}\tilde{C}_{vv}(\omega)\\ &= \frac{B}{\pi}\int_{-\infty}^{\infty}\mathrm{d}\omega\tilde{\chi}_v(\omega) = -\frac{B}{\pi}\int_{\mathrm{arc}}\mathrm{d}\omega\tilde{\chi}_v(\omega)\\ &= -\frac{B}{\pi}\lim_{R\to\infty}\int_0^{-\pi}\mathrm{d}\varphi\frac{iRe^{i\varphi}}{iRe^{i\varphi}+\tilde{\Gamma}_+(Re^{i\varphi})}\\ &= -\frac{B}{\pi}\int_0^{-\pi}\mathrm{d}\varphi = B,\end{aligned} \tag{A.5}$$

where we closed the contour in the lower half plane in which $\tilde{\chi}_v(\omega)$ has no poles due to its single-sidedness, and we assumed that $|\tilde{\Gamma}_+(z)| < \infty$ for all $z \in \mathbb{C}$. Note that in the underdamped case, *i.e.* $\tilde{\chi}(\omega) = 1/\tilde{\Gamma}_+(\omega)$, the integral diverges, since the instantaneous velocity is not defined.

Trajectory data obtained via single-particle tracking or simulation is necessarily discrete with a finite time resolution Δ. Accordingly, discrete velocity time series v_j may be obtained by differencing the position time series:

$$v_j = (x(j\Delta + \Delta/2) - x(j\Delta - \Delta/2))/\Delta. \tag{A.6}$$

We shall refer to the autocorrelation function $C_{vv,j} = \langle v_j v_0\rangle$ as the discrete VACF. We will show that the disctrete VACF can be straightforwadly obtained from the continuous MSD by taking the second central difference [38]. First note that from eq. (A.6), it follows that

$$x(j\Delta + \Delta/2) = x(\Delta/2) + \Delta\sum_{k=1}^{j} v_j. \tag{A.7}$$

Thus the MSD at time $t = j\Delta$ can be written as

$$\begin{aligned}C_{\mathrm{MSD},j} &= \left\langle (x(j\Delta+\Delta/2) - x(\Delta/2))^2\right\rangle\\ &= \left\langle\left(x(\Delta/2) + \Delta\sum_{k=1}^{j}v_k - x(\Delta/2)\right)^2\right\rangle\\ &= \Delta^2\sum_{l,k=1}^{j}\langle v_l v_k\rangle\\ &= j\Delta^2\langle v_0^2\rangle + 2\Delta^2\sum_{l=1}^{j}\sum_{k=1}^{l-1}\langle v_{l-k}v_0\rangle.\end{aligned} \tag{A.8}$$

Taking the second central difference, we obtain

$$\begin{aligned}&\frac{C_{\mathrm{MSD},j+1} - 2C_{\mathrm{MSD},j} + C_{\mathrm{MSD},j-1}}{2\Delta^2}\\ &= \sum_{k=0}^{j-1}\langle v_{j-k}v_0\rangle - \sum_{k=0}^{j-2}\langle v_{i-k-1}v_0\rangle\\ &= \langle v_j v_0\rangle = C_{vv,j}.\end{aligned} \tag{A.9}$$

Note that the discrete mean-squared velocity $\langle v_j^2\rangle = C_{vv,0}$, is given by

$$C_{vv,0} = \frac{C_{\mathrm{MSD},1}}{\Delta^2}\,, \tag{A.10}$$

where we have used that the MSD is symmetric and zero at $t = 0$.

Appendix B. Frequency domain memory kernel

Here we discuss the frequency domain representation of the delta-exponential and bi-exponential kernels as well as the constraints on their parameter values that ensure that they remain positive, as mentioned in the main text. The delta exponential kernel eq. (20) reads in the frequency domain

$$\tilde{\Gamma}(\omega) = 2a + \frac{2b}{1+\omega^2\tau^2}\,. \tag{B.1}$$

By requiring that $\tilde{\Gamma}(\omega) > 0$ we obtain

$$a\tau^2\omega^2 + a + b > 0. \tag{B.2}$$

Together with the requirement of a positve integral over the kernel, $a + b = \tau_m^{-1} > 0$, see eq. (5) in the main text, this leads to $a > 0$, *i.e.* a positive delta contribution. For the bi-exponential kernel eq. (30), we obtain in the frequency domain

$$\tilde{\Gamma}(\omega) = \frac{2a}{1+\omega^2\tau_1^2} + \frac{2b}{1+\omega^2\tau_2^2}\,, \tag{B.3}$$

which together with the requirement $\tilde{\Gamma}(\omega) > 0$ leads to

$$(a\tau_2^2 + b\tau_1^2)\omega^2 + a + b > 0. \tag{B.4}$$

It is sufficient for the inequality to hold if together with $a + b = \tau_m^{-1} > 0$, the shorter contribution of the kernel is positive, *i.e.* $\tau_2 > \tau_1$ for $a > 0$ and vice versa.

Appendix C. Generation of sample trajectories

In the following, we describe our method to generate sample trajectories of a Gaussian random walk for a given MSD. The discrete VACF, *i.e.* the autocorrelation of the discrete velocity time series $C_{vv,n} = \langle v_n v_0 \rangle$, can be obtained via eq. (A.9). Taking the discrete Fourier transform (DFT)

$$\tilde{C}_{vv,k} = \sum_{n=0}^{N-1} C_{vv,n} e^{-2\pi i k n/N}, \tag{C.1}$$

a time series of discrete velocities may be generated in the frequency domain via

$$\tilde{v}_k = \tilde{\xi}_k \sqrt{\tilde{C}_{vv,k}}. \tag{C.2}$$

Here, $\tilde{\xi}_k$ is the DFT of a realization of zero-mean, white Gaussian noise and thus $\langle \tilde{\xi}_k \tilde{\xi}_l \rangle = N \delta_{0,k+l}$. The discrete time domain velocity may then be obtained via the back-transform, $v_n = N^{-1} \sum_{k=0}^{N-1} e^{2\pi i k n/N} \tilde{v}_k$, which recovers the discrete VACF

$$\begin{aligned} \langle v_n v_0 \rangle &= \frac{1}{N^2} \sum_{k,l=0}^{N-1} e^{2\pi i k n/N} \langle \tilde{\xi}_k \tilde{\xi}_l \rangle \sqrt{\tilde{C}_{vv,k} \tilde{C}_{vv,l}} \\ &= \frac{1}{N} \sum_{k=0}^{N-1} e^{2\pi i k n/N} \tilde{C}_{vv,k} = C_{vv,n}. \end{aligned} \tag{C.3}$$

In the last step, we used the symmetry of the VACF, $\tilde{C}_{vv,k} = \tilde{C}_{vv,-k}$. The position time series $x(n\Delta + \Delta/2)$ may then be obtained via summation of v_n, see eq. (A.7).

Appendix D. Extraction of the memory kernel from correlation functions

It can be shown [44,46], that the time domain VACF and the memory kernel $\Gamma(t)$ are related via

$$C(t) - C(0) = -\int_0^t \mathrm{d}t' G(t-t') C(t'), \tag{D.1}$$

where $G(t) = \int_0^t \mathrm{d}t' \Gamma(t')$.

Given a discrete VACF of a freely diffusing particle, the corresponding memory kernel can be extracted iteratively. We discretize eq. (D.1) using the trapezoidal rule for the convolution integral:

$$C_{vv,n} - C_{vv,0} = -\frac{\Delta}{2} \sum_{i=0}^{n-1} G_{n-i-1/2} (C_{vv,i+1} + C_{vv,i}). \tag{D.2}$$

Here, the sample points of the integrated kernel $G_{n+1/2}$ are located in between the sample points of the discrete VACF $C_{vv,n}$. Equation (D.2) can then be solved iteratively:

$$\begin{aligned} \Delta G_{n+1/2} = &-2 \frac{C_{vv,n+1} - C_{vv,0}}{C_{vv,1} + C_{vv,0}} \\ &- \sum_{i=1}^{n} \Delta G_{n-i+1/2} \frac{C_{vv,i+1} + C_{vv,i}}{C_{vv,0} + C_{vv,1}}. \end{aligned} \tag{D.3}$$

From this, the discrete memory kernel Γ_i can then be obtained:

$$\begin{aligned} \Gamma_i &= \frac{G_{i+1/2} - G_{i-1/2}}{\Delta}, \\ \Rightarrow \quad \Gamma_0 &= \frac{2 G_{1/2}}{\Delta}. \end{aligned} \tag{D.4}$$

The expression for Γ_0 follows using the anti-symmetry of $G_{i+1/2}$.

In the case of overdamped dynamics, the instantaneous velocity diverges, *i.e.* $C_{vv}(0) = \infty$. In the discrete case however, $C_{vv,0}$ is always finite, see eq. (A.10). This sets an effective inertial time scale

$$\tau_m^{\mathrm{eff}} = \frac{D}{C_{vv,0}}, \tag{D.5}$$

which allows for the extraction of the kernel even for overdamped dynamics: While B and τ_m are not uniquely defined in the overdamped case, the rescaled kernel $\tau_m \Gamma(t)$ can be obtained via $\tau_m^{\mathrm{eff}} \Gamma_i$.

References

1. R. Zwanzig, Phys. Rev. **124**, 983 (1961).
2. H. Mori, Prog. Theor. Phys. **33**, 423 (1965).
3. T.G. Mason, D.A. Weitz, Phys. Rev. Lett. **74**, 1250 (1995).
4. J. Fricks, L. Yao, T.C. Elston, M.G. Forest, SIAM J. Appl. Math. **69**, 1277 (2009).
5. S.A. McKinley, L. Yao, M.G. Forest, J. Rheol. **53**, 1487 (2009).
6. T. Indei, J.D. Schieber, A. Córdoba, E. Pilyugina, Phys. Rev. E **85**, 021504 (2012).
7. M. Ernst, T. John, M. Guenther, C. Wagner, U.F. Schaefer, C.-M. Lehr, Biophys. J. **112**, 172 (2017).
8. A.M. Berezhkovskii, L. Dagdug, S.M. Bezrukov, Biophys. J. **106**, L09 (2014).
9. D. Panja, J. Stat. Mech.: Theory Exp. **2010**, L02001 (2010).
10. T. Saito, T. Sakaue, Phys. Rev. E **92**, 012601 (2015).
11. C. Maes, S.R. Thomas, Phys. Rev. E **87**, 022145 (2013).
12. H. Vandebroek, C. Vanderzande, J. Stat. Phys. **167**, 14 (2017).
13. T. Saito, T. Sakaue, Phys. Rev. E **95**, 042143 (2017).

14. O.F. Lange, H. Grubmüller, J. Chem. Phys. **124**, 214903 (2006).
15. I. Horenko, C. Hartmann, C. Schütte, F. Noe, Phys. Rev. E **76**, 016706 (2007).
16. D. de Sancho, A. Sirur, R.B. Best, Nat. Commun. **5**, 4307 (2014).
17. F. Peruani, L.G. Morelli, Phys. Rev. Lett. **99**, 010602 (2007).
18. C. Bechinger, R. Di Leonardo, H. Löwen, C. Reichhardt, G. Volpe, G. Volpe, Rev. Mod. Phys. **88**, 045006 (2016).
19. Étienne Fodor, M.C. Marchetti, Physica A **504**, 106 (2018).
20. P. Bohec, F. Gallet, C. Maes, S. Safaverdi, P. Visco, F. van Wijland, EPL **102**, 50005 (2013).
21. E. Fodor, M. Guo, N.S. Gov, P. Visco, D.A. Weitz, F. van Wijland, EPL **110**, 48005 (2015).
22. R.R. Netz, J. Chem. Phys. **148**, 185101 (2018).
23. R. Metzler, J.-H. Jeon, A.G. Cherstvy, E. Barkai, Phys. Chem. Chem. Phys. **16**, 24128 (2014).
24. I.M. Sokolov, Soft Matter **8**, 9043 (2012).
25. T. Li, M.G. Raizen, Ann. Phys. **525**, 281 (2013).
26. H.K. Shin, C. Kim, P. Talkner, E.K. Lee, Chem. Phys. **375**, 316 (2010).
27. H. Lei, N.A. Baker, X. Li, Proc. Natl. Acad. Sci. U.S.A. **113**, 14183 (2016).
28. J.O. Daldrop, B.G. Kowalik, R.R. Netz, Phys. Rev. X **7**, 041065 (2017).
29. D. Lesnicki, R. Vuilleumier, A. Carof, B. Rotenberg, Phys. Rev. Lett. **116**, 147804 (2016).
30. G. Jung, M. Hanke, F. Schmid, J. Chem. Theory Comput. **13**, 2481 (2017).
31. J. Kappler, J.O. Daldrop, F.N. Brünig, M.D. Boehle, R.R. Netz, J. Chem. Phys. **148**, 014903 (2018).
32. J. Kappler, V.B. Hinrichsen, R.R. Netz, Eur. Phys. J. E **42**, 119 (2019).
33. R. Zwanzig, *Nonequilibrium Statistical Mechanics* (Oxford University Press, 2001).
34. R. Morgado, F.A. Oliveira, G.G. Batrouni, A. Hansen, Phys. Rev. Lett. **89**, 100601 (2002).
35. J. Berner, B. Müller, J.R. Gomez-Solano, M. Krüger, C. Bechinger, Nat. Commun. **9**, 999 (2018).
36. J. Zausch, J. Horbach, M. Laurati, S.U. Egelhaaf, J.M. Brader, T. Voigtmann, M. Fuchs, J. Phys.: Condens. Matter **20**, 404210 (2008).
37. M. Krüger, F. Weysser, M. Fuchs, Eur. Phys. J. E **34**, 88 (2011).
38. B.G. Mitterwallner, C. Schreiber, J.O. Daldrop, J.O. Rädler, R.R. Netz, Phys. Rev. E **101**, 032408 (2020).
39. H.C. Berg, *E. coli in Motion* (Springer New York, 2004).
40. H.G. Othmer, S.R. Dunbar, W. Alt, J. Math. Biol. **26**, 263 (1988).
41. G. Szamel, Phys. Rev. E **90**, 012111 (2014).
42. C. Maggi, U.M.B. Marconi, N. Gnan, R. Di Leonardo, Sci. Rep. **5**, 10742 (2015).
43. E. Fodor, C. Nardini, M.E. Cates, J. Tailleur, P. Visco, F. van Wijland, Phys. Rev. Lett. **117**, 038103 (2016).
44. B.J. Berne, G.D. Harp, *On the calculation of time correlation functions*, in *Advances in Chemical Physics* (Wiley-Blackwell, 2007) pp. 63–227.
45. J.O. Daldrop, J. Kappler, F.N. Brünig, R.R. Netz, Proc. Natl. Acad. Sci. U.S.A. **115**, 5169 (2018).
46. B. Kowalik, J.O. Daldrop, J. Kappler, J.C.F. Schulz, A. Schlaich, R.R. Netz, Phys. Rev. E **100**, 012126 (2019).
47. J.H. van Zanten, K.P. Rufener, Phys. Rev. E **62**, 5389 (2000).
48. N. Corngold, Phys. Rev. A **6**, 1570 (1972).
49. T.S. Chow, J.J. Hermans, J. Chem. Phys. **56**, 3150 (1972).
50. R.R. Netz, Phys. Rev. E **101**, 022120 (2020).
51. B. Müller, J. Berner, C. Bechinger, M. Krüger, New J. Phys. **22**, 023014 (2020).